Observations from Direct UV Written, Non-Hydrogen Loaded, Thermally Regenerated Bragg Gratings in Double Clad Photosensitive Fiber

ALEXANDER JANTZEN[1,*], REX H. S. BANNERMAN[1], SAM A. BERRY[1], JAMES C. GATES[1], PAUL C. GOW[1], LEWIS J. BOYD[2], PETER G. R. SMITH[1], AND CHRISTOPHER HOLMES[1]

[1] Optoelectronics Research Centre, University of Southampton, Southampton, SO17 1BJ, United Kingdom
[2] Parker Hannifin Corporation, 2510 The Quadrant, BS32 4AQ, Bristol, United Kingdom
[*] Corresponding author: A.Jantzen@soton.ac.uk

Compiled August 18, 2017

In this paper, experimental evidence is provided for an enhanced thermal sensitivity for a double thermal regeneration feature in fiber Bragg gratings fabricated by direct ultraviolet writing. 47 gratings of varying fluence and wavelength were written along a double clad, germanium doped core fiber. Subsequently thermal processing without hydrogen loading the fiber was made and thermal treatment was done in a pure oxygen environment. Thermal sensitivity for the double regeneration increased from 13.6 ± 0.3 pm/°C to 21.3 ± 0.2 pm/°C. Furthermore, one of the highest nominal fluence gratings, #45, exhibited a regeneration factor of 1.73.

OCIS codes: *(060.3735) Fiber Bragg gratings; (060.2370) Fiber optic sensors; (060.4230) Multiplexing; (280.6780) Temperature; (120.0280) Remote sensing and sensors.*

http://dx.doi.org/10.1364/ao.XX.XXXXXX

The pursuit for sensors with high sensitivity, greater operating ranges and enhanced longevity is a continuous effort and recent advances in the field of high temperature optical interrogation has seen thermally regenerated gratings become a significant contender for harsh environment sensing[1–3]. Some of the main drivers behind regenerative gratings are the immunity to electromagnetic interference, incredible thermal resilience and the capacity for spectral multiplexing[4]. These traits allow for uses in otherwise inhospitable environments and can, with sensors, acquire crucial parameters for the optimization of performance. Significant hurdles are still being addressed, such as mechanical fragility[5], grating insertion loses[6, 7], long term stability[8] and particularly understanding the optimal fabrication conditions to regenerate the gratings[9, 10]. Once overcome in a single unified technique, thermally Regenerative Fiber Bragg gratings (RFBG) could see wider adoption within the harsh sensing community.

A good body of literature on the mechanisms governing RFBG's exist, but due to the complex nature of the formation and interlinking parameters, much research has been limited to empirical testing. The current consensus is that through the implantation of a seed grating into the core of a fiber and subsequent thermal processing, a more permanent index modulation can be obtained through stress relaxation and changes in the otherwise amorphous silica structure at higher temperatures. Hydrogen loading prior to seed grating writing, i.e. normal Fiber Bragg Grating (FBG) inscription, helps with the increase of the index contrast and thus the quality of the final grating, but is not essential for the formation of stabilized regenerated gratings[4][11].

A number of techniques for fabricating FBGs exist with the dominant method relying on the use of phase masks and pulsed exposure to either ultraviolet (UV) or infrared (IR). In addition, fibers written may require loading with hydrogen in a pressurized container at over 100 bar for several days prior to the writing. Different to these approaches, this paper outlines results achieved through the uses of a small spot ($\phi \simeq 8$ µm) Direct Ultraviolet Writing (DUW) approach using a frequency doubled Argon-ion UV continuous wave (CW) laser at 244 nm[12]. In addition to this, double clad fiber with a doped core and inner clad, was used. This configuration can be seen in figure 1. In

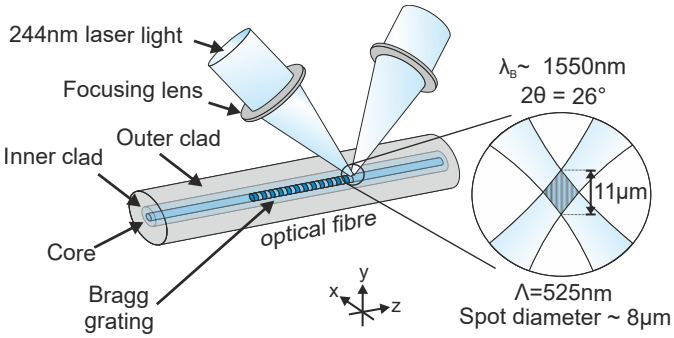

Fig. 1. Direct Ultraviolet Writing technique uses an 8 μm interferometric spot aligned to the side of the 4 μm fiber core, which is then translated along the fiber by an air-bearing stage system to generate Bragg gratings.

DUW one of the beam paths propagates through an electro-optic modulator (EOM) which allows for control over the interference pattern by varying the effective path length. This level of control means that grating period spacing can be detuned from the inherent period of interference and can therefore be used to define any Bragg wavelength within a 250 nm range[12].

For the work presented, hydrogen loading was not used prior to writing nor during the thermal processing. Photosensitive germanium doped core fiber (Nufern, GF4A) was used to avoid the need for hydrogen loading, to maintain compatibility with previous work and is conducive to small spot DUW[13]. The classification system currently used for distinguishing different types of FBGs works well for phase masks and point-to-point techniques, but is less applicable for gratings obtained through DUW. The FBGs described in this paper behave as a transitioning mix between type I and I*n* (previously known as IIa[14]). As the grating is continuously written, with each index modulation period defined in a matter of milliseconds, the typical roll over of grating growth and Bragg wavelength shift with continued exposure cannot be observed. As the regular manner of classifying gratings are based upon spectral observations during writing and/or processing environment, it is problematic to define the type for this technique because we cannot observe a shift in wavelengths[14]. Indeed for us, each fluence is a whole new grating. Higher nominal fluence gratings were found to exhibit traits more similar with type I*n* than common type I when comparing thermal performance with that reported by others for type I*n*[15]. As the writing technique focuses down to a small single spot of the two beams, a high continuous power density of 120 kW/cm^2 was used. Unique to FBGs written by DUW is the way in which it can multiplex a vast number of gratings with apodization and low insertion loss into a single fiber, thereby raising the number of independent sensing points. A series of 47 FBGs were written with a fixed laser power of 60 mW while increasing nominal fluence from; 0.1, 0.2, 0.5, 1, 2 kJcm^{-2} and then increasing in increments of 1 up to a final fluence of 44 kJcm^{-2}. This was achieved by lowering the fiber translation speed through the small writing spot. Prior to writing, the fiber was chemically stripped of its acrylic coating with acetone and isopropyl and suspended between two fiber groove clamps with 0.5 N of tension. The tension reduces the amount of sag that the horizontal fiber experiences while the writing stage translates the core through the writing spot. The combination of the 4 µm core and 8 µm writing spot meant that alignment of the fiber and its trajectory is critical to ensuring high quality gratings. This was achieved by mapping the start, middle and end position of the fiber core along the fiber length. These points were then used to fit a second order polynomial function in elevation and a linear function in horizontal for navigation. 6 mm gratings were written along the fiber and the translation velocity was slowed for each successive grating to increase nominal exposure. Gratings were written in ascending wavelength order to allow for easier identification during the in situ scan, although a quasi-random order would be preferred for decoupling the effect of detuning.

Once written, the fiber was spliced to SMF-28 and connected to a 50 : 50 coupler. A broadband S-LED source (Amonics ASLD-CWDM-5B-FA) covering 1250 to 1650 nm and an Optical Spectrum Analyser (OSA, ANDO AQ6317B) was used to interrogate the reflection spectrum. The second output, outside the furnace (Seven Thermal Solutions CU2006), was terminated into free space with index matching gel to avoid interference effects. Starting at a room temperature of 21 °C, a ramp rate was set to 5 °C/min with a dwell of 30 minutes at 850 °C. The furnace would subsequently cool at 5 °C/min down to 500 °C after which the temperature profile follows a Newtonian cooling profile. A flow of 2.0 ± 0.2 liters/min of 100% oxygen was used to purge the 1 metre long, 100 mm diameter furnace for 10 minutes prior to the run and throughout the processing. The region of fiber with gratings was placed in the uniform heating zone that spans 30 cm around the centre of the furnace. A spectral range from 1450 to 1600 nm on medium sensitivity was collected every 24 seconds by an OSA and data logged onto a computer, thus providing a temperature measurement for every 2 °C temperature increase. Spectral resolution of 0.02 nm was used as a reasonable trade-off between grating definition and scan speed. Each scan would subsequently be logged together with the temperature readings from the thermocouple to the computer. For reference and to normalize the signals, an end-facet Fresnel reflection of ∼ 4% was obtained from a freshly cleaved end, prior to thermal processing. A separate reference scan was taken from the end of a fiber coupler after thermal processing and no significant shift in source output power or spectral range was observed. The series of 47 gratings' response to the thermal processing can be seen in figure 2 along with the original reflection spectrum of the FBG prior to annealing.

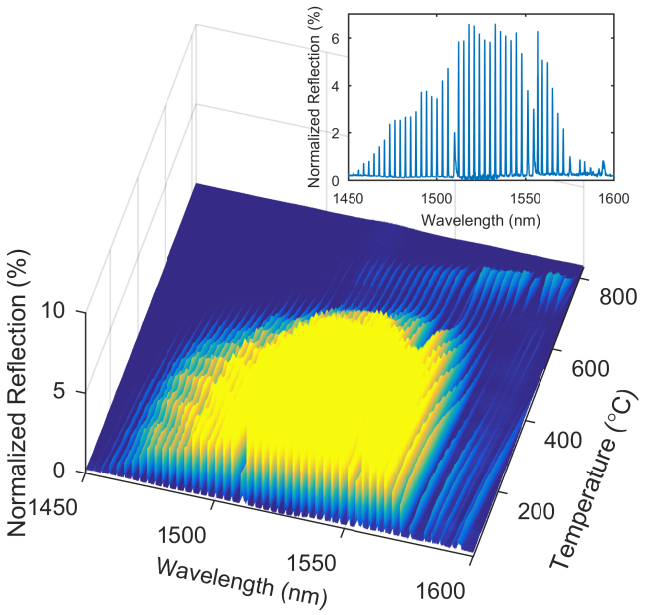

Fig. 2. Normalized reflection spectrum from 1450 to 1600 nm covering 47 direct UV written Bragg gratings with increasing nominal fluence and their corresponding temperature evolution from 20 to 840 °C. Top right figure shows the initial reflection spectrum prior to thermal annealing.

It is clear that the gratings written in the central region of the fiber yielded the strongest initial reflection despite not having been written at the highest nominal fluence. This is predominantly attributed to two reasons; the effect of DUW detuning and stage drift causing slight misalignment as it moves along the fiber[12]. Intermediate dips in the center were associated with dust particles collecting on the surface of the fiber during writing. Visual inspection post write revealed that at either extremes of the fiber, the beam focus was situated slightly below the core in

the cladding. This in effect reduced the fluence level in the core and as a result the magnitude of the index modulation. Despite the extremities exhibiting similar levels of defocusing, those written at a higher nominal fluence interestingly displayed a very different response at elevated temperatures. For all gratings, an expected red shift in Bragg wavelength was observed as temperature was increased. The reflection strength was observed to increase initially for some gratings, while for the majority it remained constant up to 180 °C. Post this temperature, a noted decline is observed for all gratings, with the gratings at the ends of the fiber trending to a minimum nearing 400 °C. The lower nominal fluence gratings do not regenerate in strength, in line with type I behaviour, while for the higher nominal fluence a slight increase is seen only briefly before turning to a second minimum at 650 °C. This minimum is shared with all other gratings as well and marks the beginning of the second thermal regeneration. Only gratings with nominal fluence greater than 19 kJ/cm^2 exhibited a regeneration in this region and a trend of increasing regeneration strength was seen with increasing nominal fluence. Further to this, a distinct increase in thermal response was observed during the second thermal regeneration and this becomes more clear when observing the higher nominal fluence gratings in figure 3. A steady shift in Bragg grating wavelength is seen up to the second minimum upon which the degree of thermal response changes.

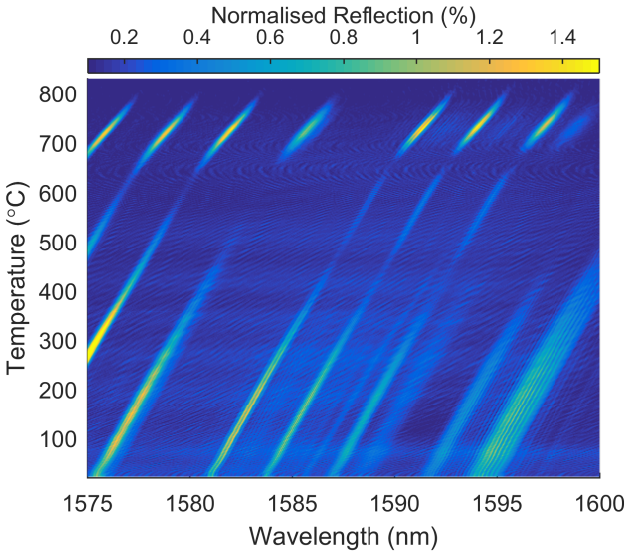

Fig. 3. High nominal fluence gratings at the end of the spectrum between 1575 and 1600 nm exhibit two regenerations phases and a marked increase in thermal response for the second thermal regeneration can be observed.

To obtain the shift in grating position, each spectral sweep was broken into regions around each grating's location. Fitting a Gaussian function to the peak allowed for the amplitude, Bragg wavelength and grating bandwidth to be extracted. Comparing the Bragg shift between successive data sets for individual gratings, a rolling thermal response is realized. Averaging the response over the number of gratings with a second thermal regeneration present, figure 4, is obtained with standard deviation marked in grey. As the thermal expansion coefficient of bulk silica increases with temperature, a slight initial increase in thermal response can be attributed to this. As temperatures approaches that of the second thermal regeneration, a sharp increase in response can be seen. This peaks at 716 ± 2 °C with a maximum thermal response, $\frac{d\lambda}{dT}$, of 21.3 ± 0.2 pm/°C. From the initial averaged grating response of 13.6 ± 0.3 pm/°C, this is an increase in thermal response to 156%. Typically reported in literature for single clad fiber is a near linear to quadratic response of the wavelength shift with temperature [4, 8, 10]. Continuing the thermal processing caused the gratings to be annealed out as reflection amplitude dropped in strength to below the noise floor and as such tracking of the gratings stopped. This can be seen in

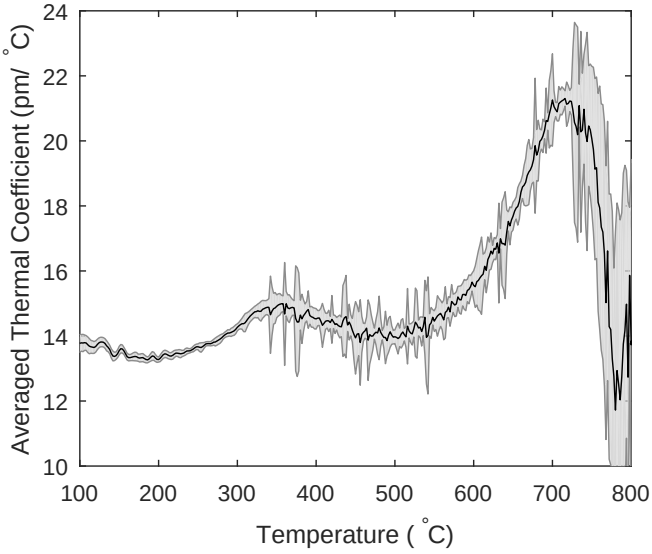

Fig. 4. Rolling thermal response averaged from gratings 22 to 46 with the shaded area denominating the standard deviation of each thermal coefficient. Two peaks are observed with crests at 350 and 716 °C.

figure 5 which shows the evolution of the reflection amplitude for grating #45. The original seed grating was observed from 20 to 475 °C, here called phase (a) with a minimum nearing 400 °C for the high nominal fluence gratings. The first regeneration is observed during phase (b) marked by the region 475 to 676 °C. This regeneration is not very strong and, in particular for gratings with high initial reflection strength, is hard to observe as the original seed gratings had not completely diminished. The second thermal regeneration is observed starting at 676 °C with a peak near 716 °C. This double regeneration is particularly clear when considering the 45th grating written with a nominal fluence of 42 kJ/cm^2.

Fitting the thermal response of each region, three coefficients are obtained and can be seen in figure 6 along with error that represents their respective 95% confidence bounds of the fit. Following the Bragg peak's central wavelength, the temperature response for the individual grating can be seen to behave in a near linear fashion up to the point of the second thermal regeneration. The increase in thermal response during phase (b) seems too large to be accounted for by changes in the thermal expansion coefficient. This would mean some other mechanism is causing it and this is supported by the occurrence of regeneration in that same region. When comparing to phase (c), it is beyond doubt that the thermal response increase is linked to the regeneration as both this and amplitude recovery are observed across the gratings simultaneously. Based upon the current theory of grating transfer from the core to the cladding boundary

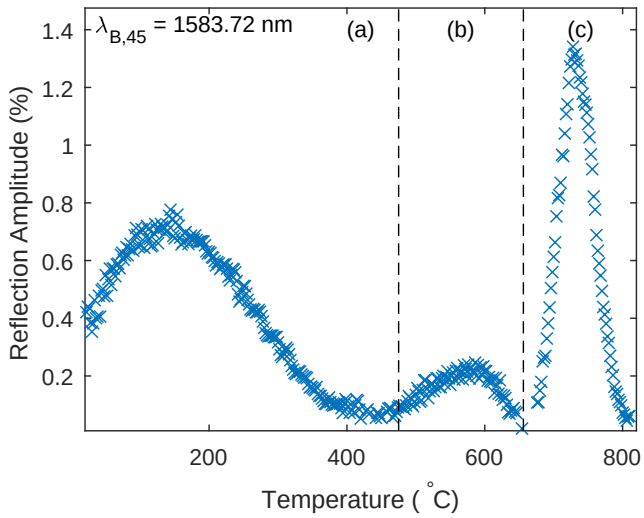

Fig. 5. Reflection amplitude temperature evolution of Bragg grating #45. Sectioned into three regions; (a) seed grating: 20 to 475 °C, (b) first regeneration: 475 to 656 °C and (c) second thermal regeneration: 656 to 820 °C.

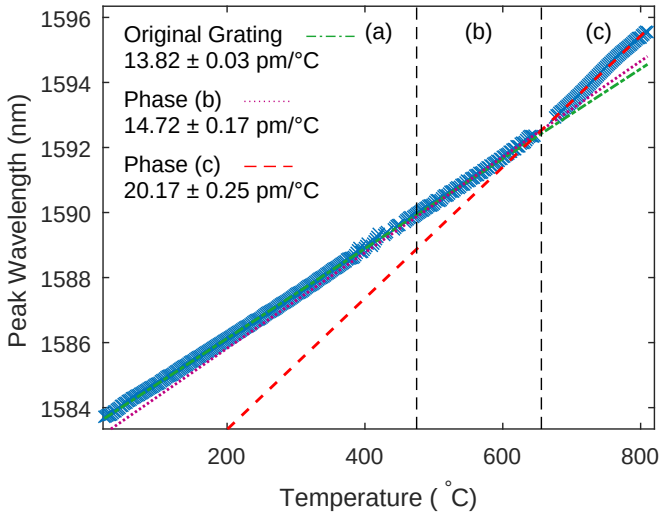

Fig. 6. Bragg grating #45 peak shift as temperature is increased with regeneration regions marked and respective gradients evaluated. Noteworthy is the sharp increase in thermal response between region (a) and (c) to 146%.

interface during the thermal annealing, it would be reasonable to advocate that this is further evidenced. In this case, the presence of a double clad structure is observed by the presence of the double regeneration. It should be noted that the observation of secondary grating growth has been reported in literature, albeit without the simultaneous enhanced thermal sensitivity[11][15]. Different to this work, was the use of multiple heating steps rather than the continuous ramp tested here. As the inner clad only constitutes a fraction of the cross section, the interface effect is less pronounced than the transfer into the main outer clad. The enhancement in thermal response in this case could be linked to boundary stresses due to differing dopant concentrations between clads and core. A separate consideration that has to be made is also the effect of the DUW method upon the final regeneration. From figure 2 a correlation between nominal writing fluence and the relative regeneration strength exists while the effect of spot position remains unknown. As the regeneration strength for the higher nominal fluence off center gratings is greater than the initial seed grating, there is scope for using this technique for obtaining compact RFBG that no longer exhibit weakening of the reflection amplitude. Mechanical strength is still a profound problem of fibers annealed at this temperature, however, the answer to this may lay with more engineering based approaches such as Integrated Optical Fiber (IOF)[13]. A combination of DUW RFBG and IOF could prove a strong contender for a stable, harsh environment optical sensing.

In summary, this paper has reported the experimental observation of double regeneration of DUW gratings with higher nominal fluence and the enhancement of thermal sensitivity from $\mathbf{13.6} \pm \mathbf{0.3}$ pm/°C to $\mathbf{21.3} \pm \mathbf{0.2}$ pm/°C. This was done in an oxygen rich environment with the presence of no hydrogen during writing nor annealing. An increase of reflection from the seed grating to the final grating with a regeneration factor of 1.73 was also observed in the case for high nominal fluence gratings and has the potential for overcoming one of the current challenges with RFBG in terms of weakening reflection strength. As gratings were annealed beyond their maximum temperature, no comparison between initial seed, first and second thermal regeneration gratings was possible at room temperature.

FUNDING INFORMATION

We thank the Engineering and Physical Sciences Research Council (EPSRC) (EP/M508147/1, EP/M024539/1, EP/M013243/1, EP/M013294/1, EP/K034480/1) and Fluid Systems Division of Parker Aerospace, part of the Parker Hannifin Corporation, for supporting this work.

REFERENCES

1. J. Canning, Measurement: Journal of the International Measurement Confederation **79**, 236 (2016).
2. J. Kumar, O. Prakash, R. Mahakud, S. K. Agrawal, S. K. Dixit, S. V. Nakhe, and J. Canning, Sensors and Actuators B: Chemical **244**, 54 (2017).
3. B. T. Górriz, I. Payá-Zaforteza, P. A. C. García, and S. S. Maicas, Sensors and Actuators A: Physical **254**, 116 (2017).
4. E. Lindner, C. Chojetztki, S. Brueckner, M. Becker, M. Rothhardt, J. Vlekken, and H. Bartelt, Sensors **9**, 8377 (2009).
5. S. J. Mihailov, Sensors **12**, 1898 (2012).
6. D. Grobnic, C. A. Hnatovsky, and S. J. Mihailov, Optics Express **24**, 28704 (2016).
7. S. J. Mihailov, D. Grobnic, R. B. Walker, C. A. Hnatovsky, H. Ding, D. Coulas, and P. Lu, Proc. SPIE **9852**, 98520F (2016).
8. M. Celikin, D. Barba, B. Bastola, A. Ruediger, and F. Rosei, Optics Express **24**, 21897 (2016).
9. P. Holmberg, F. Laurell, and M. Fokine, Optics Express **23**, 27520 (2015).
10. J. He, Y. Wang, C. Liao, C. Wang, S. Liu, K. Yang, Y. Wang, X. Yuan, G. P. Wang, and W. Zhang, Scientific Reports **6**, 23379 (2016).
11. E. Lindner, C. Chojetzki, S. Brückner, M. Becker, M. Rothhardt, and H. Bartelt, Optics Express **17**, 12523 (2009).
12. C. Sima, J. C. Gates, H. L. Rogers, P. L. Mennea, C. Holmes, M. N. Zervas, and P. G. R. Smith, Optics Express **21**, 15747 (2013).
13. S. G. Lynch, C. Holmes, S. A. Berry, J. C. Gates, A. Jantzen, T. I. Ferreiro, and P. G. R. Smith, Optics Express **24**, 8391 (2016).
14. J. Canning, Laser and Photonics Reviews **2**, 275 (2008).
15. E. Lindner, J. Canning, C. Chojetzki, S. Brückner, M. Becker, M. Rothhardt, and H. Bartelt, Optics Communications **284**, 183 (2011).

FULL REFERENCES

1. J. Canning, "Regeneration, regenerated gratings and composite glass properties: The implications for high temperature micro and nano milling and optical sensing", Measurement: Journal of the International Measurement Confederation **79**, 236-249 (2016).

2. J. Kumar, O. Prakash, R. Mahakud, S. k. Agrawal, S. K. Dixit, S. V. Nakhe, and J. Canning, "Wavelength independent chemical sensing using etched thermally regenerated FBG", Sensors and Actuators B: Chemical **244**, 54-60 (2017).

3. B. T. Górriz, I. Payá-Zaforteza, P. A. C. García, and S. S. Maicas, "New fiber optic sensor for monitoring temperatures in concrete structures during fires", Sensors and Actuators A: Phyiscal **254**, 116-125 (2017).

4. E. Lindner, C. Chojetztki, S. Brückner, M. Becker, M. Rothhardt, J. Vlekken, and H. Bartelt, "Arrays of Regenerated Fiber Bragg Gratings in Non-Hydrogen-Loaded Photosensitive Fibers for High-Temperature Sensor Networks", Sensors **9**, 8377-8381 (2009).

5. S. J. Mihailov, "Fiber bragg grating sensors for harsh environments", Sensors **9**, 1898-1918 (2009).

6. D. Grobnic, C. A. Hnatovsky, and S. J. Mihailov, "Low loss Type II regenerative Bragg gratings made with ultrafast radiation", Optics Express **24**, 28704-28712 (2016).

7. S. J. Mihailov, D. Grobnic, R. B. Walker, C. A. Hnatovsky, H. Ding, D. Coulas, and P. Lu, "New technique for fabrication of low loss high temperature stable high reflectivity FBG sensor arrays", Proc. SPIE **9852**, 98520F (2016).

8. M. Celikin, D. Barba, B. Bastola, A. Ruediger, and F. Rosei, "Development of regenerated fiber Bragg grating sensors with long-term stability", Optics Express, **24**, 21897-21909 (2016).

9. P. Holmberg, F. Laurell, and M. Fokine,"Influence of pre-annealing on the thermal regeneration of fiber Bragg gratings in standard optical fibers", Optics Express **23**, 27520-27535 (2015).

10. J. He, Y. Wang, C. Laio, C. Wang, S. Liu, K. Yang, Y. Wang, X. Yuan, G. P. Wang, and W. Zhang, "Negative-index gratings formed by femtosecond laser overexposure and thermal regeneration", Scientific Reports **6**, 23379-23388 (2016).

11. E. Lindner, C. Chojetzki, S. Brückner, M. Becker, M. Rothhardt, and H. Bartelt, "Thermal regeneration of fiber Bragg gratings in photosensitive fibers", Optics Express **17**, 12523-12531 (2009).

12. C. Sima, J. C. Gates, H. L. Rogers, P. L. Mennea, C. Holmes, M. N. Zervas, and P. G. R. Smith, "Ultra-wide detuning planar Bragg grating fabrication technique based on direct UV grating writing with electro-optic phase modulation", Optics Express **21**, 15747-15754 (2013).

13. S. G. Lynch, C. Holmes, S. A. Berry, J. C. Gates, A. Jantzen, T. I. Ferreiro, and P. G. R. Smith, "External cavity diode laser based upon an FBG in an integrated optical fiber platform", Optics Express, **24**, 8391-8398 (2016).

14. J. Canning, "Fibre gratings and devices for sensors and laser", Laser and Photonics Reviews, **4**, 275-289 (2008).

15. E. Lindner, J. Canning, C. Chojetzki, S. Brückner, M. Becker, M. Rothhardt, and H. Bartlet, "Thermal regenerated type IIa fiber Bragg gratings for ultra-high temperature operation", Optics Communications, **284**, 183-185 (2011).